Phospholipase C-Induced Aggregation and Fusion of Cholesterol–Lecithin Small Unilamellar Vesicles†

Andrew S. Luk,‡ Eric W. Kaler,*,‡ and Sum P. Lee§

Center for Molecular and Engineering Thermodynamics, Department of Chemical Engineering, University of Delaware, Newark, Delaware 19716, and VA Medical Center, Seattle, Washington 98108

Received February 5, 1993; Revised Manuscript Received April 15, 1993

ABSTRACT: We have investigated the effects of the Ca^{2+}-requiring enzyme phospholipase C on the stability of sonicated vesicles made with different molar ratios of cholesterol to lecithin. Vesicle aggregation is detected by following turbidity with time. Upon the addition of phospholipase C and after a short lag period, the turbidity of a vesicle dispersion increases continuously with time. The rate of increase of turbidity increases with both the enzyme-to-vesicle ratio and the cholesterol content of the vesicles. Vesicle fusion and leakage of contents are monitored by a contents-mixing fusion assay using 8-aminonaphthalene-1,3,6-trisulfonic acid (ANTS) and *p*-xylylenebis(pyridinium bromide) (DPX) as the fluorescence probes [Ellens, H., Bentz, J., & Szoka, F. C. (1985) *Biochemistry 24*, 3099–3106]. The results clearly show that phospholipase C induces vesicle fusion. The rate of vesicle fusion correlates with the enzyme-to-vesicle ratio but not with the cholesterol content of the membrane. Negligible aggregation and fusion of vesicles occurs when the experiment is repeated with buffer free of Ca^{2+}. The membrane-destabilizing diacylglycerol, a product of lecithin hydrolysis by phospholipase C, is speculated to play a major role in driving the observed vesicle aggregation and fusion. The kinetics of vesicle aggregation and vesicle fusion can be predicted by linking Michaelis–Menten enzyme kinetics to a mass-action model.

Cholesterol is relatively insoluble in water ($\sim 10^{-8}$ M), but cholesterol is solubilized in bile to millimolar levels by bile salt–lecithin mixed micelles and lecithin vesicles (Sömjen & Gilat, 1985; Lee et al., 1987; Carey, 1988). Mixed micelles of bile salt and lecithin are rodlike in shape, with the lecithin arranging radially along the rod axis and the bile salts shielding the hydrophobic portions of the lecithin at both ends of the rod (Hjelm et al., 1990). Vesicles are spherical closed bilayers of lecithin containing little or no bile salt (Mazer & Carey, 1983; Sömjen et al., 1986; Lee et al., 1987). Cholesterol is solubilized by interdigitating into the hydrophobic region of these microstructures. In hepatic bile under conditions of low bile salt secretion, vesicles exist as the predominant cholesterol carriers. When hepatic bile is secreted to the gall bladder, additional micellar particles are formed via a dynamic interchange of lecithin from vesicles to free bile salts or existing mixed micelles. This process increases the net cholesterol-to-lecithin ratio in the remaining vesicles (Carey & Cohen, 1987; Little et al., 1991). The resultant cholesterol-enriched vesicles are thermodynamically metastable, and are likely the precursors to cholesterol gallstone formation (Lee et al., 1987).

The equilibrium phase diagram for model bile constructed by Carey and Small (1978) shows that at low cholesterol concentration, bile salt micelles and bile salt–lecithin mixed micelles are the primary cholesterol carriers. In bile supersaturated with cholesterol, vesicles are the major cholesterol vehicles. As equilibrium is approached, cholesterol (CH)[1] nucleates and forms CH monohydrate crystals. Both *in vivo* and *in vitro* studies show that nucleating cholesterol originates almost exclusively from the vesicles (Lee et al., 1987; Peled et al., 1988; Lee & Sekijima, 1991). On the basis of video-enhanced contrast microscopy, this vesicle-to-crystal transition can be described by a series of stages (Halpern et al., 1986). First, cholesterol-rich vesicles undergo a series of aggregation, and possibly fusion, steps. The clustering of these vesicle aggregates produces large multivesicular particles. Cholesterol then begins to nucleate, and the resultant microcrystals undergo a subsequent period of crystal growth into macroscopic cholesterol aggregates. Such aggregates are presumably the precursors of cholesterol gallstones.

The metastability of bile is often quantified in terms of nucleation time. Because cholesterol crystals are birefringent, they are uniquely visible with a polarizing microscope. Nucleation time is defined as the time taken for a sample of precentrifuged and crystal-free bile to produce microscopically evident solid cholesterol crystal (Holan et al., 1979). Several factors (e.g., bile salt-to-lecithin ratio, total lipid concentration, and degree of cholesterol supersaturation) affect nucleation time by altering the cholesterol-to-lecithin ratio of the vesicles (Kibe et al., 1985). However, normal human bile is frequently supersaturated with cholesterol (Holzbach et al., 1973). Thus, cholesterol supersaturation alone is not the sole driving force in accelerating nucleation, and the prolonged stability of the cholesterol-rich vesicles in normal bile must depend on factors other than cholesterol content. For example, high protein concentrations in human bile have been associated with the presence of cholesterol crystals (Strasberg et al., 1990). From clinical investigations, several proteins, such as mucin (Levy et al., 1984), phospholipases (Nakano et al., 1988; Pattison & Willis, 1991a), and immunoglobulins (Harvey et al., 1991), have been identified in human gall bladder bile. These proteins

† Supported in part by the Whitaker Foundation and by Grant DK-41678 from the National Institutes of Health. S.P.L. is supported in part by the Medical Research Service of the Department of Veterans Affairs.

* Author to whom correspondence should be addressed.

‡ University of Delaware.

§ VA Medical Center.

[1] Abbreviations: CH, cholesterol; L, egg lecithin; PLC, phospholipase C; ANTS, 8-aminonaphthalene-1,3,6-trisulfonic acid; DPX, *p*-xylylenebis(pyridinium bromide); DAG, diacylglycerol; PC, phosphatidylcholine; PE, phosphatidylethanolamine; PS, phosphatidylserine; HEPES, *n*-(2-hydroxyethyl)piperazine-*N*′-2-ethanesulfonic acid; SUV, small unilamellar vesicle(s); LUV, large unilamellar vesicle(s); E/V, enzyme-to-vesicle ratio.

0006-2960/93/0432-6965$04.00/0

shorten the time for cholesterol nucleation, and are thus termed pro-nucleating agents. Conversely, some anti-nucleating agents, such as apolipoprotein A-I and apolipoprotein A-II, prolong the nucleation time (Kibe et al., 1984; Tao et al., 1993).

Phospholipase C (PLC) is a potential pro-nucleating agent in human gall bladder bile (Pattison, 1988; Pattison & Willis, 1991b). PLC, which requires calcium ion as a cofactor, hydrolyzes the phosphoester bond of lecithin and concomitantly yields the water-insoluble diacylglycerol and the headgroup phosphorylcholine. Diacylglycerol (DAG) is known to stimulate lateral phase separation in a mixture of phospholipids (Ortiz et al., 1988), destabilize lipid membranes (Dawson et al., 1984; Das & Rand, 1984, 1986), and induce membrane fusion (Ellens et al., 1989; Siegel et al., 1989). DAG also activates phospholipases (Dawson et al., 1983) and plays a major role in various biochemical cellular processes (Berridge, 1984). Previously, Groen et al. (1989b) have identified an important factor that promotes cholesterol nucleation and also binds to a concanavalin A–Sepharose column. This so-called Con A-binding protein is resistant to Pronase treatment and shifts cholesterol preferentially to the vesicular phase in model bile. Interestingly, PLC activity is present in this Con A-binding factor (Pattison & Willis, 1991b). Nevertheless, the significance of PLC to the pathogenesis of cholesterol gallstone disease remains unclear (Groen et al., 1989a).

Membrane fusion is central to various biochemical processes such as cell fusion, exocytosis, and endocytosis. Liposome or phospholipid vesicle fusion can be divided into two distinct mechanisms: divalent cation-induced fusion of negatively charged phospholipid (e.g., PS) vesicles (Wilschut et al., 1980) and temperature-induced fusion of polymorphic lipid (e.g., PE) vesicles (Bentz & Ellens, 1988). DAG is speculated to induce vesicle fusion involving the transient existence of nonbilayer fusion intermediates (Siegel et al., 1989) as is the case for fusion of PE-containing vesicles. PLC, possibly through the effect of DAG, induces the fusion of both large and small unilamellar vesicles composed of phosphatidylcholine (PC), phosphatidylethanolamine (PE), and cholesterol (CH) (Nieva et al., 1989, 1993; Burger et al., 1991; Little et al., 1992).

Knowledge of the kinetics of cholesterol nucleation is currently based entirely on determination of the qualitative parameter of nucleation time. Since the experimental resolution of light microscopy is above ca. 1 μm, nucleation time is a measure of the overall process of cholesterol crystallization. This measurement certainly does not examine the molecular-scale process of nucleation *per se*, but is confounded by other variables such as crystal growth (Busch et al., 1990). No systematic study has been performed to determine the kinetics of the events preceding cholesterol nucleation. Vesicle aggregation is an essential step preceding nucleation, so pro-nucleating proteins must have a strong impact on the metastability of cholesterol–lecithin vesicles. In order to understand the process of cholesterol nucleation at a molecular level, we report here the effects of the putative pro-nucleating agent PLC on the aggregation and fusion of sonicated small unilamellar vesicles containing cholesterol and lecithin. The use of sonicated small unilamellar CH–L vesicles as a model of biliary processes is already well established (Stark et al., 1985; Little et al., 1991; Lichtenberg et al., 1988). The overall process of vesicle aggregation and vesicle fusion is probed by absorbance/turbidity measurements, while a fluorescence fusion assay is employed to investigate vesicle fusion alone (Ellens et al., 1985). The observed kinetics of aggregation and fusion of cholesterol–lecithin vesicles can be predicted by coupling enzyme kinetics and mass-action models. In comparison to the observations of Nieva et al. (1989, 1993), we have extended the study of PLC-induced vesicle fusion to cholesterol–lecithin SUV and have determined the effects of PLC concentration and cholesterol vesicular content on the rate of vesicle aggregation and fusion through a rigorous kinetics model. Such kinetic studies contribute to the functional and quantitative analysis of protein–lipid interactions and help in the understanding of gallstone pathogenesis.

MATERIALS AND METHODS

Phospholipase C (EC 3.1.4.3) (PLC) of highest purity from *Clostridium perfringens* was purchased from Sigma (St. Louis, MO) and used as received (SDS–PAGE molecular mass was 35 kDa). Cholesterol (CH) and egg yolk lecithin (L) were obtained from Sigma and used without further purification. 8-Aminonaphthalene-1,3,6-trisulfonic acid (ANTS) and *p*-xylylenebis(pyridinium bromide) (DPX) were purchased from Molecular Probes (Eugene, OR). Water used was distilled and deionized, and all glassware was acid-washed.

Small unilamellar vesicles composed of cholesterol and lecithin or of lecithin alone were prepared using the method of Huang (1969) with minor modification. Cholesterol and lecithin mixtures were prepared in various molar ratios (approximately 1:1, 1:2, 1:4) by coprecipitation from chloroform. The solvent was evaporated by a stream of nitrogen in a rotary evaporator, and the residual solvent was eliminated thoroughly under vacuum. The dried lipid was resuspended in the appropriate buffer. The hydrated lipid solutions were sparged with argon and directly sonicated (Heat Systems Ultrasonics Model W-225) in an ice–water bath for 90 min. Sonicated dispersions were centrifuged at 25 °C for 2 h at 32000*g*, and the top three-fourths of the supernatant was collected and incubated overnight at 25 °C. The mean hydrodynamic radius of the vesicles was measured by quasi-elastic light scattering (Berne & Pecora, 1976). The samples were discarded if not used on the following day.

Vesicle fusion was determined by a contents-mixing and leakage assay using ANTS/DPX as the fluorescence probes (Ellens et al., 1985). Small unilamellar vesicles were prepared in solutions of either (a) 25 mM ANTS, 80 mM NaCl, 5 mM $CaCl_2$, and 5 mM HEPES, (b) 90 mM DPX, 40 mM NaCl, 5 mM $CaCl_2$, and 5 mM HEPES, or (c) 12.5 mM ANTS, 45 mM DPX, 60 mM NaCl, 5 mM $CaCl_2$, and 5 mM HEPES. The vesicles were separated from unencapsulated material by gel filtration on a Sephadex G-75 column, using 0.15 M NaCl, 5 mM $CaCl_2$, and 5 mM HEPES as the elution buffer. All of the above buffer solutions were adjusted to pH 7.0, and were checked to be isosmotic (Osmotte A, Precision Instruments). To inhibit bacteria growth, 0.02 wt % of NaN_3 was added to each buffer. The total volume was set to 2.5 mL, and the final lecithin concentration was 0.5 mM [except at the highest enzyme-to-vesicle ratio (E/V), for which the final lecithin concentration was 0.3 mM]. Both the size of cholesterol–lecithin vesicles and the number of lecithin molecules per vesicle depend on the cholesterol content. Thus, at fixed lecithin concentration, the initial number density of vesicles will be different for each cholesterol composition. To compare the kinetics of changes of vesicles with different cholesterol contents, the appropriate reference parameter is the amount of phospholipase C per vesicle (E/V). Phospholipase C was added with initial stirring to ensure uniform distribution to the vesicle dispersion, but no mechanical stirring was imposed during the experiment to mimic the quiescent environment in the gall bladder.

Fluorescence measurements were performed with a Perkin-Elmer MPF-66 spectrofluorometer. Excitation was set at 355 nm, and emission was measured at 530 nm with the addition of a 430-nm filter to eliminate scattered light. The fluorescence signal measured was corrected for the inner-filter effect as given by Lakowicz (1983),[2] and the small fluorescence signal due to the enzyme alone was subtracted from the measured intensities. Vesicle fusion was registered as a decrease in ANTS fluorescence due to collisional quenching by DPX. The 100% fluorescence level (or 0% fusion) was set by using a 1:1 mixture of ANTS and DPX vesicles at the final desired lecithin concentration. The 100% fusion level (or 0% leakage) was given by the fluorescence intensity of vesicles coencapsulating both ANTS and DPX at the final lecithin concentration. The 100% leakage level was obtained by lysing the coencapsulated vesicles with 3 mM Triton X-100.

Vesicle aggregation was monitored by following the absorbance at 300 nm in a Perkin-Elmer Lambda 2 spectrophotometer at room temperature. Vesicles were prepared by sonication with the elution buffer, and the same buffer solution without vesicles was used as a reference. To maintain the consistency of the absorbance and fluorescence protocols, the vesicle dispersion was also passed through a Sephadex G-75 column equilibrated with the same elution buffer. The final lecithin concentration used in each run was identical to the corresponding run in the fluorescence assay. Lipid phosphorus was determined by a modification of the method of Bartlett (1959), and the cholesterol content was determined by a cholesterol oxidase assay (Allain et al., 1974).

THEORY

Vesicle aggregation and vesicle fusion are characterized with the following mass-action kinetic model:

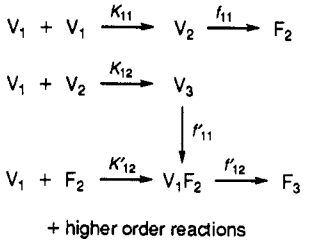

(1)

where V_1 denotes a sonicated vesicle, V_i ($i > 1$) denotes vesicle aggregates, F_j ($j > 1$) denotes fused vesicle aggregates, V_iF_j denotes the prefusion aggregates, K_{ij} represents the second-order rate constant for aggregation, and f_{ij} represents the first-order rate constant for fusion. Detailed derivations of the rate equations for different aggregates are available (Bentz & Nir, 1981; Nir et al., 1980). In order to simplify the model, two assumptions are made. First, the rate constants for all higher order reactions are considered equivalent; thus, $K_{ij} = K'_{ij} = K_{11} = K$ and $f_{ij} = f'_{ij} = f_{11} = f_o$. The final constants K and f_o thus represent respectively the average rate of aggregation and fusion of the lipid vesicles. Second, vesicle aggregation is assumed to be an irreversible process. Vesicle disaggregation is not negligible for systems that exhibit considerable reversible aggregation such as divalent cation-induced vesicle fusion, but because of the nonelectrostatic nature of the DAG-driven vesicle aggregation, the extent of disaggregation in our system is expected to be small. Since the focus of our study is on aggregation and fusion, the rate of disaggregation will be lumped into the aggregation rate constant K. The modified kinetic model then has two parameters, K and f_o, and the two parameters can be obtained from the two independent experiments monitoring absorbance and fluorescence. The theory has been developed completely for analysis of the kinetics of vesicle fusion from a fluorescence fusion experiment (Nir et al., 1980; Düzgüneş & Bentz, 1988), including the correction of the fluorescence fusion signal due to leakage of encapsulated contents (Nir et al., 1983).

Vesicle aggregation is commonly probed by monitoring the increase in absorbance or turbidity associated with the increase in the intensity of light scattered by larger aggregates. From light-scattering principles, the intensity scattered from a vertically polarized light source by a dilute solution of small spherical particles can be described in the Rayleigh–Gans–Debye approximation (Berne & Pecora, 1976) as

$$I_\theta/I_o = A(\lambda, V_s, n)[N_p]P(\theta) \qquad (2)$$

where I_θ/I_o is the scattered light intensity at a scattering angle θ relative to the incident intensity, A is a constant that depends on several experimental parameters (the wavelength of light λ, the volume of the particle V_s, and the particle refractive index n), $[N_p]$ is the number density of the scattering particles, and $P(\theta)$ is the particle form factor. For a dilute solution of polydisperse particles, the total scattered intensity is given by the sum of the intensities scattered by individual particles. Since the absorbance is a function of the total intensity scattered by a given sample at all angles, the absorbance at any time can be calculated by integrating eq 2 over all angles:

$$\frac{I_s(t)}{I_o} = 1 - 10^{-\mathrm{Abs}(t)} = A\sum_{i=1}^{M} i^2[N_i(t)]\int_0^{2\pi} P_i(\theta)\sin\theta\,(1+\cos^2\theta)\,d\theta \qquad (3)$$

where $I_s(t)/I_o$ is the total scattered intensity, Abs(t) denotes the absorbance at time t, i is the degree of aggregation, M is the largest aggregate considered, and $[N_i(t)]$ and $P_i(\theta)$ represent respectively the number density and the form factor of the ith aggregate. The term $1 + \cos^2\theta$ results from the use of unpolarized light in the spectrophotometer. The form factor of a vesicle is known (Berne & Pecora, 1976), and all higher order aggregates are assumed to be vesicular in shape. Aggregates with the same overall degree of aggregation are treated identically (e.g., V_3, F_3, and V_1F_2 are all treated as trimers). The vesicle bilayer width is assumed to be 35 Å, and the headgroup area is obtained by interpolation between

[2] Due to the sample turbidity, both the incident excitation intensity and the observed emitting fluorescence intensity are weakened. This phenomenon is known as the inner-filter effect. The attenuation of the final fluorescence intensity can be approximately corrected by

$$I_{corr} \approx I_{obs}\,\mathrm{antilog}\left(\frac{\mathrm{Abs}_{ex} + \mathrm{Abs}_{em}}{2}\right)$$

where I_{obs} represents the observed fluorescence intensity and Abs_{ex} and Abs_{em} denote the absorbance or the optical density of the sample at the excitation and emission wavelengths, respectively. The absorbance of the sample at any time is obtained from a parallel experiment of vesicle aggregation under the same conditions. When a fluorescence fusion assay is performed with ANTS vesicles and blank vesicles (with no quencher but plain buffer), the observed fluorescence intensity decreases substantially due to the increasing turbidity of the vesicle dispersion (results not shown). For the ANTS/DPX assay, the use of raw data will lead to overestimation of the extent of ANTS quenching by DPX and thus the rate of vesicle fusion. On the other hand, for the pair of fluorophores terbium (Tb^{3+}) and dipicolinic acid (DPA), vesicle fusion is indicated by fluorescence enhancement upon their complex formation (Wilschut et al., 1980). By the same token, the presence of the inner-filter effect will in this case lead to the underestimation of the rate of vesicle fusion. The discrepancy between the results obtained from the two assays has been noted by Düzgüneş and Bentz (1988).

70 Å^2 for pure lecithin and 96 Å^2 for lecithin in a 1:1 molar mixture of cholesterol and lecithin (Lis et al., 1982). The total lecithin concentration thus sets the number density of the initial monodisperse vesicle population, and the sizes of the higher order aggregates are computed with the constraint that the lipid volume be conserved.

Unlike most cation-induced fusion of negatively charged phospholipid vesicles, the increase in absorbance in PLC-induced vesicle fusion proceeds only after a lag period (see below). Since a lag period is observed, aggregation is not instantaneous, and the aggregation rate constant K depends on time. If DAG is the principal cause of PLC-induced vesicle fusion, the rate of aggregation will depend on the amount of DAG produced. As a first approximation, the aggregation rate constant K is assumed to depend linearly on the mole percentage of DAG in the outer monolayer of the vesicle, and DAG flip-flop is assumed to be slow on the time scale of the experiment. The rate of DAG production in turn is predicted by simple Michaelis–Menten enzyme kinetics with the measured values of $V_{max} \approx 1.0 \times 10^{-4}$ mM s^{-1} and $K_M \approx 0.018$ mM as obtained by Patterson (1988). In this view, the second-order aggregation rate constant is time-dependent and given by

$$K(t) = k_o \left\{ \frac{[DAG]}{[L(t = 0)]} \right\}_{\text{outer monolayer}} \quad (4)$$

with the concentration of DAG calculated from

$$\frac{d[DAG]}{dt} = -\frac{V_{max}[L]_{out}}{K_M + [L]_{out}} \quad (5)$$

where k_o is the proportionality constant (M^{-1} s^{-1}) and [L(t = 0)] is the initial concentration of lecithin in the outer monolayer of the membrane. The final model is therefore characterized by the two key parameters k_o and f_o.

Because this two-parameter model is highly nonlinear, the fitting procedure is iterative. A first guess for k_o is obtained by first fitting a simple single-parameter mass-action model (Nir et al., 1980) to the experimental absorbance curve. Holding k_o constant, the experimental data from the fluorescence assay are then fitted to the complete model to acquire f_o. Successive absorbance/fluorescence fittings are repeated until the rate constants k_o and f_o converge. The model results are insensitive of M for values above 7, and M was set equal to 8 for all of the fits.

RESULTS

Addition of PLC causes the absorbance of a vesicle dispersion to increase with time (Figure 1). The initial absorbance rise is not instantaneous, but proceeds after a lag time. The lag period diminishes with increasing enzyme concentration and cholesterol content. The rate of vesicle aggregation also increases with the PLC-to-vesicle ratio. Similar phenomena were observed by Nieva et al. (1989) using large unilamellar vesicles composed of PC/PE/CH. The fluorescence assay detects fusion in all vesicles tested. Contrary to the observations of Nieva et al. (1989), pure lecithin vesicles do undergo both aggregation and fusion in the presence of PLC, and vesicle fusion occurs with concomitant leakage of vesicle contents (Figure 2). The rate of fluorescence quenching (expressed as the percent of maximum fluorescence) and the rate of vesicle leakage both increase with E/V. Since leakage of vesicles leads to underestimation of the extent of vesicle fusion, a correction for leakage is necessary in order to express vesicle fusion on an absolute

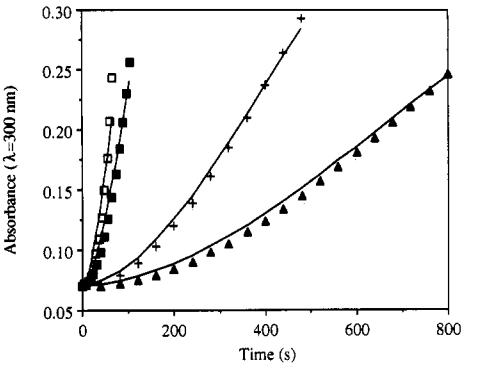

FIGURE 1: Aggregation of cholesterol–lecithin SUV (36 mol % CH) induced by phospholipase C is shown over time by the light absorbance at 300 nm. A buffered solution with no vesicles is used as reference. Four enzyme loadings are used and are expressed as enzyme-to-vesicle ratio (E/V): (□) 7; (■) 1; (+) 0.1; (▲) 0.02. For all cases other than $E/V = 7$, the lecithin concentration used is 0.5 mM, while for $E/V = 7$, the lecithin concentration used is 0.3 mM. The solid lines show the fits given by the coupled enzyme kinetics–mass-action model.

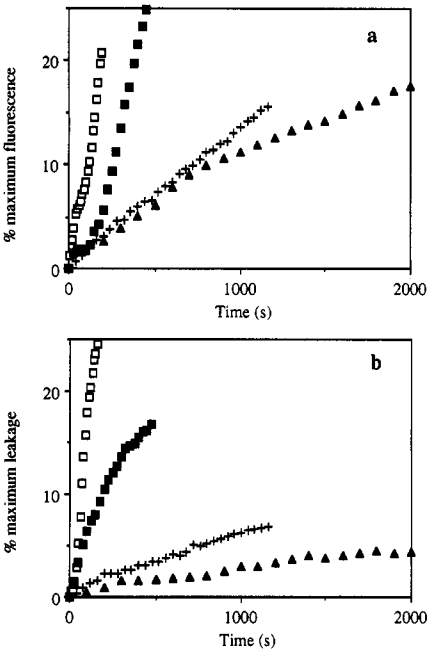

FIGURE 2: (a) Phospholipase C-induced fusion of cholesterol–lecithin vesicles (36 mol % CH) as probed by ANTS/DPX fluorescence fusion assay is shown over time. Data are not corrected for vesicle leakage. (b) Leakage of internal contents during vesicle fusion is shown over time (36 mol % CH). Data for both figures are corrected for turbidity as described under Materials and Methods. Symbols for E/V are used as in Figure 1. The lecithin concentration used is identical to that in the absorbance experiment. Excitation is set at 355 nm, and emission is monitored at 515 nm.

scale in terms of the percent of maximum fusion (Figure 3). Surprisingly, the increase in the fusion signal does not proceed after a lag period. Similar fluorescence curves with no lag time are obtained for all vesicles. Likewise, no lag time is detected for the PLC-induced fusion of PC/PE/CH (50:25:25) small unilamellar vesicles (Nieva et al., 1989).

The solid lines in Figures 1 and 3 show the theoretical fits generated by the coupled enzyme kinetics–mass-action model. The fitting quality is insensitive to a wide range of enzyme parameters, V_{max} and K_M. The model precisely predicts vesicle aggregation with the presence of a lag period (Figure 1). Since aggregation is the precursor to fusion, the fluorescence fit based on the mass-action model also yields a lag time comparable to that of the absorbance data. The discrepancy

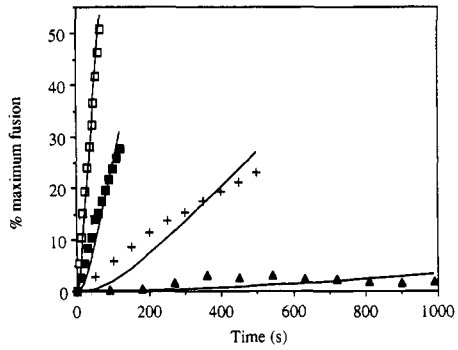

FIGURE 3: Fusion of cholesterol–lecithin SUV (50 mol % CH) expressed as percent maximum fusion is shown over time. The experimental data are corrected for turbidity and for vesicle leakage during fusion (see Theory). Symbols for E/V are identical as in previous figures. The solid lines represent the fits given by the model.

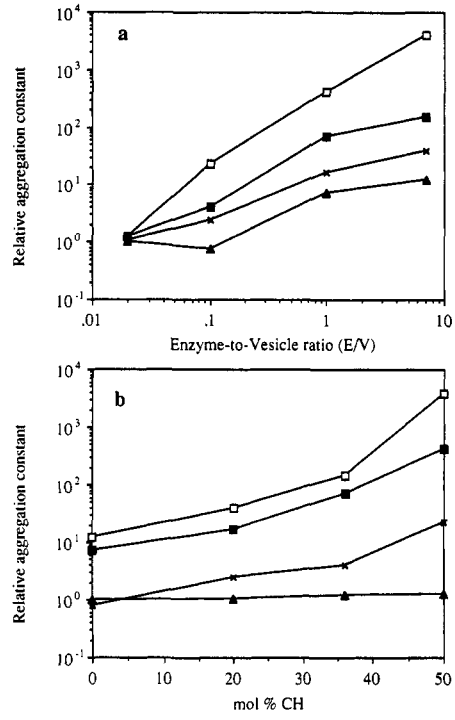

FIGURE 4: Fitted second-order aggregation proportionality rate constants, k_o, for all experiments relative to the fitted rate constant obtained for fusion of pure lecithin vesicles at an E/V of 0.02 are plotted ($k_o/k_{o[\text{pure L, } E/V=0.02]}$) versus (a) E/V for vesicles with different mole percent CH: (□) 50; (■) 36; (×) 20; (▲) 0 (pure lecithin); and (b) CH mole percent in vesicles for different E/V: (□) 7; (■) 1; (×) 0.1; (▲) 0.02.

in the prediction of vesicle fusion at low enzyme concentrations originates from the loss of the experimental lag time due to the necessary corrections made on the measured fluorescence intensity (Figure 3). Because f_o describes inherently the tendency of the bilayer to fuse after vesicle adhesion, the fitted numerical value of f_o is only slightly affected by the loss of the lag period in the fluorescence data.

The two parameters k_o and f_o computed from the model fits are summarized in Figures 4 and 5. Enzyme activity was proved positive by a colorimetric assay (Krug et al., 1979); however, the assay is not sufficiently quantitative for the accurate acquisition of V_{max} and K_M. Since the enzyme parameters are not available, constant and approximate values of V_{max} and K_M from *in vivo* study of phospholipase C (Pattison, 1988) are used for all cases. In turn, the absolute second-order rate constant K is a function of V_{max} and k_o (see eq 4 and 5), and at low DAG production, K is approximately

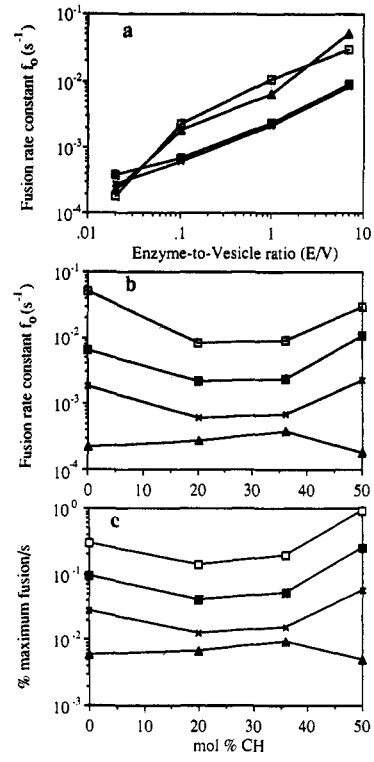

FIGURE 5: (a) Fitted first-order fusion rate constants (f_o) for all cases are plotted versus E/V for vesicles with different mole percent CH. (b) Fitted fusion rate constants are plotted versus CH mole percent in vesicles for different E/V. Symbols used are the same as in Figure 4a,b. (c) Rate of fusion in terms of percent maximum fusion per second is plotted versus mole percent CH.

proportional to the product of k_o and V_{max} at all times. Since V_{max} scales linearly with enzyme concentration and depends on the cholesterol content in the bilayer, the fitted k_o does not correspond to an absolute value when V_{max} is assumed constant for all cases. In order to sort out the effects of cholesterol content and E/V on K, the relative proportionality aggregation constant, which is defined as the ratio of each fitted k_o to that obtained from the fusion of pure lecithin vesicles at the lowest E/V (0.02), serves as a reference parameter and is plotted in Figure 4. In other words, the dimensionless relative aggregation rate constant provides a comparison of k_o obtained at different experimental conditions. The proportionality rate constant k_o clearly scales with the amount of PLC present (Figure 4a) and increases with the cholesterol content in the bilayer (Figure 4b).

The fusion rate constant f_o, on the other hand, is assumed to be independent of the rate of DAG production (but not of the overall concentration of DAG in the membrane), and thus it is obtained on an absolute scale. Similarly, f_o increases with E/V (Figure 5a), but f_o does not scale linearly with cholesterol content. f_o exhibits a minimum at a cholesterol: lecithin ratio of approximately 1:4 except at the lowest E/V (Figure 5b). The overall rate of vesicle fusion is often expressed as the initial slope of the experimental corrected fluorescence curve in terms of the percent maximum fusion per second. The slope of the experimental curve and the theoretical fusion rate constant f_o are obtained independently from the data, but behave similarly with respect to bilayer cholesterol content (Figure 5b,c). Since the overall rate of vesicle fusion is affected by both k_o and f_o, the similar behavior of f_o and the percent maximum fusion per second is to be expected, and this agreement further confirms that f_o is a valid measure of the tendency for the lipid bilayer to undergo fusion after aggregation.

The above experiments were selectively repeated with Ca^{2+}-free buffer, and negligible vesicle aggregation and fusion were observed (results not shown). Moreover, all vesicle dispersions of interest are stable in the absence of PLC. Vesicle aggregation and fusion hence are induced by the membrane DAG and not by any hydrophobic or electrostatic effects exerted by either PLC or Ca^{2+} alone.

DISCUSSION

The formation of cholesterol gallstones in human bile is a slow and complex process. Biliary cholesterol supersaturation is a necessary but not sufficient condition to cause gallstone formation in humans. In the lithogenic process, the metastable cholesterol-rich vesicles undergo aggregation, then fusion, and ultimately nucleation of cholesterol crystals. The stability of biliary vesicles decreases with increasing cholesterol content in the bilayer and with the presence of pro-nucleating agents. Since cholesterol nucleation depends on a balance between the activity of various pro-nucleating and anti-nucleating agents, it is of utmost importance to quantify the kinetics of aggregation and fusion of cholesterol–lecithin vesicles induced by individual agents. In a previous study by our group, PLC-induced fusion of CH–L (1:1) vesicles was observed by transmission electron microscopy, and the resultant vesicle growth was monitored on the basis of quasi-elastic light scattering (Little et al., 1992). In this study, we have quantitatively detected and characterized both aggregation and fusion of cholesterol–lecithin small unilamellar vesicles induced by the pro-nucleating agent phospholipase C.

A lag time is present in each PLC-induced CH–L vesicle aggregation curve. This delay time decreases with increasing E/V and increasing cholesterol content of the vesicles. Similar lag times have been noted in the PLC-induced fusion of LUV composed of PC/PE/CH, and the duration of the lag period varies with membrane composition and enzyme concentration (Nieva et al., 1989). On the other hand, the fluorescence signal changes instantaneously in cation-induced fusion of vesicles containing negatively charged PS (Wilschut et al., 1980). It is likely that the lag time originates from the properties of the fusogenic proteins (Bentz & Ellens, 1988; Hong et al., 1991). The protein may drive vesicle fusion by physical forces, such as charge neutralization or local dehydration of the lipid surface, without chemically modifying the lipid membrane. In such cases, the lag time indicates the presence of a rate-determining binding step. Conversely, the protein (or enzyme) may modify the lipid membrane chemically to produce new fusogenic lipid molecules with entirely different physical properties, in which case the rate of fusion gradually increases while membrane products are accumulating. In PLC-mediated fusion, the membrane-destabilizing product DAG builds up in the bilayer membrane while fusion proceeds, as no aggregation and fusion are observed when Ca^{2+}-free buffer is used. The lag time is abolished when the vesicles containing initially 10 mol % DAG are used (Nieva et al., 1993). Moreover, the overall DAG concentration increases with E/V, as does the fusion rate constant f_o (Figure 5a).

At a molecular level, the process of membrane fusion can be subdivided into three stages: close adhesion of apposing membranes; destabilization of membranes with concomitant exchange of membrane lipids; and mixing of internal aqueous contents (Bentz & Ellens, 1988). Close adhesion of bilayers, or vesicle aggregation, can be promoted by charge neutralization and local dehydration of bilayers. Membrane destabilization is enhanced by local defects or local fluctuations in lipid packing that exist within the merged bilayer. For instance, in cation-induced fusion of PS vesicles, divalent cations, such as Ca^{2+} and Mg^{2+}, screen the surface charges of the membrane and thus lower the electrostatic repulsion between the charged PS vesicles. Close adhesion of PS bilayers is facilitated by the formation of dehydrated complexes between Ca^{2+} and PS molecules (Papahadjopoulos et al., 1978; Bentz & Ellens, 1988).

In PLC-induced vesicle fusion, DAG is responsible for the destabilization of bilayer membranes. The underlying mechanism resembles that of the fusion of PE-containing vesicles. Unsaturated PE forms a variety of lipid phases depending on temperature, pH, and the presence of other phospholipids. For example, upon increasing temperature, hydrated PE in the liquid-crystalline lamellar phase undergoes a transition, via the inverted cubic phase, to the inverted hexagonal phase. Depending on the morphology of the phase that is stable at a given temperature, PE-containing vesicles can undergo aggregation, fusion, and contact-mediated lysis (Ellens et al., 1986a). Fusion of PE-containing vesicles only occurs within the temperature range where an isotropic ^{31}P-NMR resonance signal is present, indicating that the isotropic inverted cubic phase is important in bilayer fusion (Ellens et al., 1986b). Several mechanisms and their corresponding fusion intermediates have been proposed (Burger & Verkleij, 1990). Inverted micelles, commonly known as "type II" nonbilayer lipid intermediates or lipidic particles, are considered the important intermediates in the fusion of PE vesicles (Hope et al., 1983; Verkleij, 1984). During vesicle fusion, these short-lived inverted micelles are formed as a consequence of the local perturbations and reorganizations of lamellar packing within the interacting membranes.

DAG, like PE, has a low degree of headgroup hydration and prefers nonlamellar phases. The presence of DAG lowers the lamellar to hexagonal phase transition temperature in some pure phospholipid membranes (Das & Rand, 1984; Siegel et al., 1989). Hydrated egg phosphatidylcholine, which prefers lamellar phases at all temperatures, undergoes a lamellar-to-hexagonal isothermal phase transition when 30 mol % egg DAG is added (Das & Rand, 1986). In analogy to the mechanism of PE-containing vesicles, an isotropic ^{31}P-NMR resonance is registered when DAG is incorporated into PC membranes (Dawson et al., 1984). Moreover, isotropic ^{31}P-NMR spectra are recorded in association with the fusion of PS/PC vesicles caused by DAG (Gómez-Fernández et al., 1989). The nonlamellar DAG thus perturbs the lipid membranes and enhances the transient formation of nonbilayer intermediates. PLC therefore drives vesicle fusion through the local destabilizing effects of DAG on the cholesterol–lecithin bilayers. Nonetheless, liposomes performed with 10 mol % DAG are stable in the absence of PLC (Nieva & Alonso, 1991). On the basis of lipid packing arguments, DAG may tend to reside in the inner monolayer of these liposomes, and the fusogenic strength of DAG would thus be dramatically repressed. The local perturbation in lipid packing exerted by the penetration of PLC on the lipid bilayer may also be essential for the onset of vesicle aggregation as suggested by Nieva and Alonso (1991).

DAG causes lateral phase separation in mixed PS/PC membranes (Ohki et al., 1982), and both saturated DAG and unsaturated DAG induce lipid immiscibilities in pure dipalmitoyl-PC membranes (Ortiz et al., 1988). However, it is not clear whether phase separation is involved in the observed PLC-induced vesicle aggregation and vesicle fusion. Since PLC shortens nucleation time, the possible existence of

hydrophobic patches or microdomains of CH–DAG in large vesicular aggregates may provide the surface necessary for cholesterol nucleation.

Regarding leakage of internal contents, increasing temperature above the hexagonal phase transition temperature results in contact-mediated lysis of PE-containing vesicles (Ellens et al., 1986a). Leakage can therefore be caused by the transient formation of nonlamellar phases in the lipid bilayer. Contrary to the observations of Nieva et al. (1989), leakage is recorded in every vesicle fusion trial in this study. Since DAG mediates vesicle fusion by the transient formation of nonbilayer intermediates, the leakage of internal contents is anticipated. The extent of leakage correlates with the PLC concentration, probably due to the presence of more fusion intermediates as DAG is produced. With the same E/V, the extent of leakage also increases with increasing cholesterol content (results not shown).

Uncharged sonicated lecithin vesicles are stable for days above the gel–liquid-crystalline transition temperature (Wong & Thompson, 1982). Short-range repulsive forces, such as the "hydration" force or steric forces, act to prevent the fully hydrated lecithin vesicles from attaining close contact. When incorporated in PS vesicles, lecithin retards cation-induced aggregation and fusion either by lowering the ratio of bound Ca^{2+} per PS molecule or by turning up the short-range repulsive forces (Düzgüneş & Papahadjopoulos, 1990). Since lecithin is the major phospholipid in human bile, the prolonged metastability of biliary vesicles is not surprising. In this study, we have shown that PLC induces the aggregation and fusion of pure lecithin vesicles. Contrary to the observations of Nieva et al. (1989), the presence of DAG alone results in the dehydration of lecithin headgroups, eliminates the short-range repulsive forces, and mediates fusion of lecithin vesicles, without the presence of other fusogenic lipids such as PE or cholesterol.

At the same enzyme concentration, the rate of vesicle aggregation increases with the cholesterol content of the vesicles (Figure 4b). This rate enhancement can be due to several effects. From the colloidal point of view, cholesterol decreases the short-range steric repulsion in PC liposomes by spreading apart the lipid headgroups (McIntosh et al., 1989). Cholesterol also increases the magnitude of the long-range van der Waals attractions between membranes. The combination of both effects results in a reduction of the energy barrier necessary for the close approach of two lecithin membranes, and these effects will probably be more pronounced with the presence of the hydrophobic DAG in the membrane. In addition, depending on the cholesterol concentration in the bilayer, membrane ordering and lipid phase transitions can be altered to a substantial degree (Yeagle, 1985). For instance, the presence of cholesterol at about 20–30 mol % is postulated to induce lipid phase segregation within the cholesterol–lecithin membranes into CH-rich and L-rich microdomains. Through these membrane modifications, both the binding of PLC to the membrane and the number of available enzyme docking sites can be affected. Since enzyme activity depends on the physical form of the lipid substrates, the changes in membrane properties may affect indirectly the intrinsic rate of DAG production, and thus influence the rate of membrane destabilization.

The first-order fusion rate constant f_o does not scale with cholesterol bilayer content in a simple way (Figure 5b). For a constant E/V, f_o approaches a minimum value at a cholesterol:lecithin ratio of about 1:4 (except for $E/V = 0.02$). A similar trend is observed for the cation-induced fusion of PS vesicles (Düzgüneş & Papahadjopoulos, 1990). Since the fusion rate constant f_o indicates the tendency of the lipid bilayer to fuse after aggregation, the lecithin membrane with approximately 25 mol % cholesterol is less prone to fusion. This behavior may also be attributed to the complex concentration-dependent effects of cholesterol on lipid membrane properties. Since the transition temperature for egg lecithin is low, pure lecithin bilayers exist in the liquid-crystalline phase at 25 °C. The incorporation of cholesterol will lower the fluidity of the bilayer, which may indirectly hinder the lateral movements of lipids. During membrane fusion, the formation of fusion intermediates through lipid reorganization will therefore be retarded, resulting in a decrease in f_o. On the contrary, at higher cholesterol concentration (>20–30 mol %), the possible formation of hydrophobic CH–DAG microdomains may enhance the dehydration of two opposing monolayers. In addition, since large amounts of cholesterol facilitate the formation of inverted phases in mixed PE/PC membranes (Tilcock et al., 1982), cholesterol may similarly enhance the formation of nonbilayer fusion intermediates by DAG in lecithin membranes, leading to an increase in f_o with cholesterol content.

PLC hydrolysis of lecithin vesicles takes place entirely at the lipid–water interface of the outer monolayer, and the Michaelis–Menten model may not be appropriate for this type of interfacial catalysis. For phospholipase A_2 hydrolysis of lipid vesicles, a complete interfacial enzyme catalysis model has been constructed (Berg et al., 1991). This model assumes no exchange of bound enzymes between vesicles. The rate of enzyme hydrolysis is obtained by summing up the product formation from each individual vesicle, and depends strongly on the statistical distribution of enzymes per vesicle. In addition, the kinetics of PLC hydrolysis of lecithin can be complicated by end-product inhibition. With PC/PE/CH (50:25:25) LUV, product inhibition becomes significant when the DAG content reaches 15 mol %, as evidenced by the flattening of the experimental fluorescence curve (Nieva et al., 1993). When CH–L (50:50) SUV are used, the effect of product inhibition is not substantial until about 40% of the lecithin is hydrolyzed (Little et al., 1993). In order to ensure that product inhibition does not interfere with the analysis, only the early portions of the absorbance and fluorescence curves are used for kinetics analysis in this study. Since only the early stages of vesicle aggregation and fusion are described here, simple Michaelis–Menten kinetics are employed as a first approximation.

The observed vesicle aggregation induced by PLC is not instantaneous (Figure 1). Hence, the aggregation rate constant K must be time-dependent. Because there is continuous enzymatic production of the fusogenic DAG, in a first approximation, the aggregation rate constant K is assumed proportional to the mole fraction of DAG in the outer monolayer, and the production of DAG is obtained from the simple Michaelis–Menten kinetic model. Thus, the aggregation rate constant K is governed by both PLC activity and the tendency of the bilayer to aggregate. If V_{max} and K_M are known, the proportionality rate constant k_o will represent the tendency of the vesicles to aggregate. However, in the absence of enzyme kinetics data, the values of V_{max} and K_M obtained from *in vivo* studies are used. At low DAG content (<10%), K is approximately proportional to the product of V_{max} and k_o. Since V_{max} is kept constant, the changes in enzyme kinetics with different experimental conditions will be reflected in a change of the apparent fitted value of k_o. Despite these estimations, the above model succeeds in describing the rate

Table I: Second-Order Aggregation Rate Constant, K, at 5 mol % Lecithin Hydrolysis at 20 °C[a]

cholesterol mol % in vesicle	K (M^{-1} s^{-1}) = $0.05k_o$, phospholipase C-to-vesicle ratio			
	7	1	0.1	0.02
50	5.7×10^7	6.0×10^6	3.3×10^5	1.8×10^4
36	2.0×10^6	9.6×10^5	5.3×10^4	1.6×10^4
20	5.3×10^5	2.3×10^5	3.3×10^4	1.4×10^4
0	2.1×10^5	1.0×10^5	9.8×10^3	1.4×10^4
Smoluchowski upper limit:[b]	$\sim 7 \times 10^9$ (25 °C)			

[a] The absolute values of the second-order rate constants were calculated from the fitted k_o at the point when 5% DAG is accumulated in the bilayer. [b] The rate constant for the Smoluchowski diffusion rate-limited aggregation is given by $k_{SM} = 8kT/3\eta$ where η is the viscosity of the medium, k is the Boltzmann constant, and T is the temperature.

of absorbance increase and the overall rate of vesicle fusion. Both the quality of the fit and the resultant aggregation rate constant K are insensitive to the chosen value of V_{max}. The absolute value of K at 5 mol % DAG is thus given in Table I. In all cases, vesicle aggregation is slow in comparison to the Smoluchowski diffusion-limited aggregation.

In order to understand the physiological effect of PLC on biliary vesicles, the enzyme-to-vesicle ratio serves as an unbiased parameter to compare results between *in vitro* and *in vivo* studies. The ratio E/V *in vivo* is in the range of 10^{-2}–10^{-3}. We have shown that cholesterol–lecithin vesicles undergo aggregation and fusion even at low E/V. On the basis of the coupled enzyme kinetics and mass-action models, the experimental results for the PLC-induced aggregation and fusion of cholesterol–lecithin vesicles are accurately predicted. From the PLC-induced vesicle aggregates, we have also observed at a later time the formation of solid crystals of cholesterol monohydrate using video-enhanced contrast microscopy (unpublished experiment). Since cholesterol gallstone formation is a slow process, the significance of PLC in the pathogenesis of cholesterol gallstone disease cannot be ignored. We have, for the first time, examined the kinetics of vesicle aggregation and fusion using PLC as a "probe" nucleator. On the basis of the mass-action kinetics, the aggregation and fusion rate constants, which are independent of the initial vesicle or lipid concentration, can be employed as a direct indication of the potency of other putative pro-nucleating proteins in reducing vesicle stability. Similar approaches can be useful in dissecting the mechanistic or functional features of other pro- or anti-nucleators at a molecular level, and will ultimately lead to a better understanding of the role of proteins in the pathogenesis of cholesterol gallstone disease.

ACKNOWLEDGMENT

We are grateful for discussions with Dr. T. E. Little and for the use of Dr. A. M. Lenhoff's spectrofluorometer, and appreciate the experimental assistance of J. H. Klein.

REFERENCES

Allain, C. A., Poon, L. S., Chan, C. S. G., Richmond, W., & Fu, P. C. (1974) *Clin. Chem. 20*, 470–475.
Bartlett, G. R. (1959) *J. Biol. Chem. 234*, 466–468.
Bentz, J., & Nir, S. (1981) *Proc. Natl. Acad. Sci. U.S.A. 78*, 1634–1637.
Bentz, J., & Ellens, H. (1988) *Colloids Surf. 30*, 65–112.
Berg, O. G., Yu, B., Rogers, J., & Jain, M. K. (1991) *Biochemistry 30*, 7283–7297.
Berne, B. J., & Pecora, R. (1976) *Dynamic Light Scattering*, Wiley, New York.
Berridge, M. J. (1984) *Biochem. J. 220*, 345–360.
Burger, K. N. J., Verkleij, A. J. (1990) *Experientia 46*, 631–644.
Burger, K. N. J., Nieva, J., Alonso, A., & Verkleij, A. J. (1991) *Biochim. Biophys. Acta 1068*, 249–253.
Busch, N., Tokumo, H., & Holzbach, R. T. (1990) *J. Lipid Res. 31*, 1903–1909.
Carey, M. C. (1988) in *Bile Acids in Health and Disease* (Northfield, T., et al., Eds.) pp 61–82, Klumer Academic Publishers, Boston.
Carey, M. C., & Small, D. M. (1978) *J. Clin. Invest. 61*, 998–1026.
Carey, M. C., & Cohen, D. E. (1987) *Falk Symp. 45*, 287–300.
Das, S., & Rand, R. P. (1984) *Biochem. Biophys. Res. Commun. 124*, 491–496.
Das, S., & Rand, R. P. (1986) *Biochemistry 25*, 2882–2889.
Dawson, R. M. C., Hemington, N. L., & Irvine, R. F. (1983) *Biochem. Biophys. Res. Commun. 117*, 196–201.
Dawson, R. M. C., Irvine, R. F., Bray, J., & Quinn, P. J. (1984) *Biochem. Biophys. Res. Commun. 125*, 836–842.
Düzgüneş, N., & Bentz, J. (1988) in *Spectroscopic Membrane Probes V.I* (Loew, L. M., Ed.) pp 117–159, CRC Press, Boca Raton, FL.
Düzgüneş, N., & Papahadjopoulos, D. (1990) in *Advances in Cholesterol Research* (Esfahani, M., et al., Eds.) pp 367–384, Telford Press, Caldwell, U.K.
Ellens, H., Bentz, J., & Szoka, F. C. (1985) *Biochemistry 24*, 3099–3106.
Ellens, H., Bentz, J., & Szoka, F. C. (1986a) *Biochemistry 25*, 285–294.
Ellens, H., Bentz, J., & Szoka, F. C. (1986b) *Biochemistry 25*, 4141–4147.
Ellens, H., Siegel, D. P., Alford, D., Yeagle, P. L., Boni, L., Lis, L. J., Quinn, P. J., & Bentz, J. (1989) *Biochemistry 28*, 3692–3703.
Gómez-Fernández, J. C., Aranda, F. J., Micol, V., Villalaín, J., & Ortiz, A. (1989) *Biochem. Soc. Trans. 17*, 957–960.
Groen, A. K., Noordam, C., Drapers, J. A. G., Egbers, P., Hoek, F. J., & Tytgat, G. N. J. (1989a) *Biochim. Biophys. Acta 1006*, 179–182.
Groen, A. K., Ottenhoff, R., Jansen, P. L. M., van Marle, J., & Tytgat, G. N. J. (1989b) *J. Lipid Res. 30*, 51–58.
Halpern, Z., Dudley, M. A., Kibe, A., Lynn, M. P., Breuer, A. C., & Holzbach, R. T. (1986) *Gastroenterology 90*, 875–885.
Harvey, P. R. C., Upadhya, G. A., & Strasberg, S. M. (1991) *J. Biol. Chem. 266*, 13996–14003.
Hjelm, R. P., Alkan, M. H., & Thiyagarajan, P. (1990) *Mol. Cryst. Liq. Cryst. 180A*, 155–164.
Holan, K. R., Holzbach, R. T., Hermann, R. E., Cooperman, A. M., & Claffey, W. J. (1979) *Gastroenterology 77*, 611–617.
Holzbach, R. T., Marsh, M., Olszewski, M., & Holan, K. (1973) *J. Clin. Invest. 52*, 1467–1479.
Hong, K., Meers, P. R., Düzgüneş, N., & Papahadjopoulos, D. (1991) in *Membrane Fusion* (Wilschut, J., et al., Eds.) pp 195–208, Dekker, New York.
Hope, M. J., Walker, D. C., & Cullis, P. R. (1983) *Biochem. Biophys. Res. Commun. 110*, 15–22.
Huang, C. H. (1969) *Biochemistry 8*, 344–352.
Kibe, A., Holzbach, R. T., LaRusso, N. F., & Mao, S. J. T. (1984) *Science 225*, 514–516.
Kibe, A., Dudley, M. A., Halpern, Z., Lynn, M. P., Breuer, A. C., & Holzbach, R. T. (1985) *J. Lipid Res. 26*, 1102–1111.
Krug, F. L., Truesdale, N. J., & Kent, C. (1979) *Anal. Biochem. 97*, 43–47.
Lakowicz, J. R. (1983) *Principles of Fluorescence Spectroscopy*, pp 43–46, Plenum Press, New York.
Lee, S. P., & Sekijima, J. (1991) in *Textbook of Gastroenterology* (Yamada, T., et al., Eds.) pp 1966–1989, J. B. Lippincott Company, Philadelphia.
Lee, S. P., Park, H. Z., Madani, H., & Kaler, E. W. (1987) *Am. J. Physiol 251*, G374–G383.
Levy, P. F., Smith, B. F., & LaMont, J. T. (1984) *Gastroenterology 87*, 270–275.

Lichtenberg, D., Ragimova, S., Bor, A., Almog, S., Vinkler, C., Kalina, M., Peled, Y., & Halpern, Z. (1988) *Biophys. J. 54*, 1013–1025.
Lis, L. J., McAlister, M., Fuller, N., Rand, R. P., & Parsegian, V. A. (1982) *Biophys. J. 37*, 657–666.
Little, T. E., Lee, S. P., Madani, H., Kaler, E. W., & Chinn, K. (1991) *Am. J. Physiol. 260*, G70–G79.
Little, T. E., Madani, H., Lee, S. P., & Kaler, E. W. (1992) *J. Lipid Res. 34*, 211–217.
Mazer, N. A., & Carey, M. C. (1983) *Biochemistry 22*, 426–442.
McIntosh, T. J., Magid, A. D., & Simon, S. A. (1989) *Biochemistry 28*, 17–25.
Nakano, T., Yanagisawa, J., & Nakayama, F. (1988) *Hepatology 8*, 1560–1564.
Nieva, J., & Alonso, A. (1991) in *Progress in Membrane Biochemistry* (Gómez-Fernández, J. C., et al., Eds.) pp 177–194, Birkäuser, Verlag, Basel, Switzerland.
Nieva, J., Goñi, F. M., & Alonso, A. (1989) *Biochemistry 28*, 7364–7367.
Nieva, J., Goñi, F. M., & Alonso, A. (1993) *Biochemistry 32*, 1054–1058.
Nir, S., Bentz, J., & Wilschut, J. (1980) *Biochemistry 19*, 6030–6036.
Nir, S., Bentz, J., Wilschut, J., & Düzgüneş, N. (1983) *Prog. Surf. Sci. 13*, 1–124.
Ohki, K., Sekiya, T., Yamauchi, T., & Nozawa, Y. (1982) *Biochim. Biophys. Acta 693*, 341–350.
Ortiz, A., Villalaín, J., & Gómez-Fernández, J. C. (1988) *Biochemistry 27*, 9030–9036.
Papahadjopoulos, D., Portis, A., & Pangborn, W. (1978) *Ann. N.Y. Acad. Sci. 308*, 50–63.
Pattison, N. R. (1988) *Biochem. Biophys. Res. Commun. 150*, 890–896.
Pattison, N. R., & Willis, K. E. (1991a) *J. Lipid Res. 32*, 215–221.
Pattison, N. R., & Willis, K. E. (1991b) *Gastroenterology 101*, 1339–1344.
Peled, Y., Halpern, Z., Baruch, R., Goldman, G., & Gilat, T. (1988) *Hepatology 8*, 914–918.
Siegel, D. P., Banschbach, J., Alford, D., Ellens, H., Lis, L. J., Quinn, P. J., Yeagle, P. L., & Bentz, J. (1989) *Biochemistry 28*, 3703–3709.
Sömjen, G. J., & Gilat, T. (1985) *J. Lipid Res. 26*, 699–704.
Sömjen, G. J., Marikovsky, Y., Lelkes, P., & Gilat, T. (1986) *Biochim. Biophys. Acta 879*, 14–21.
Stark, R. E., Gosselin, G. J., Donovan, J. M., Carey, M. C., & Roberts, M. F. (1985) *Biochemistry 24*, 5599–5605.
Strasberg, S. M., Toth, J. L., Gallinger, S., & Harvey, P. R. C. (1990) *Gastroenterology 98*, 739–746.
Tao, S., Tazuma, S., & Kajiyama, G. (1993) *Biochim. Biophys. Acta 1166*, 25–30.
Tilcock, C. P. S., Bally, M. B., Farren, S. B., & Cullis, P. R. (1982) *Biochemistry 21*, 4596–4601.
Verkleij, A. J. (1984) *Biochim. Biophys. Acta 779*, 43–63.
Wilschut, J., Düzgüneş, N., Fraley, R., & Papahadjopoulos, D. (1980) *Biochemistry 19*, 6011–6021.
Wong, M., & Thompson, T. E. (1982) *Biochemistry 21*, 4133–4139.
Yeagle, P. L. (1985) *Biochim. Biophys. Acta 822*, 267–287.